

Technical University of Denmark



Structure–Activity Relationship Study of Selective Excitatory Amino Acid Transporter Subtype 1 (EAAT1) Inhibitor 2-Amino-4-(4-methoxyphenyl)-7-(naphthalen-1-yl)-5-oxo-5,6,7,8-tetrahydro-4H-chromene-3-carbonitrile (UCPH-101) and Absolute Configurational Assignment Using Infrared and Vibrational Circular Dichroism Spectroscopy in Combination with *ab Initio* Hartree–Fock Calculations

Huynh, Tri H.V.; Shim, Irene; Bohr, Henrik; Abrahamsen, Bjarke; Nielsen, Birgitte; Jensen, Anders A.; Bunch, Lennart

Published in:

Journal of Medicinal Chemistry

Link to article, DOI:

[10.1021/jm300345z](https://doi.org/10.1021/jm300345z)

Publication date:

2012

Document Version

Publisher's PDF, also known as Version of record

[Link back to DTU Orbit](#)

Citation (APA):

Huynh, T. H. V., Shim, I., Bohr, H., Abrahamsen, B., Nielsen, B., Jensen, A. A., & Bunch, L. (2012). Structure–Activity Relationship Study of Selective Excitatory Amino Acid Transporter Subtype 1 (EAAT1) Inhibitor 2-Amino-4-(4-methoxyphenyl)-7-(naphthalen-1-yl)-5-oxo-5,6,7,8-tetrahydro-4H-chromene-3-carbonitrile (UCPH-101) and Absolute Configurational Assignment Using Infrared and Vibrational Circular Dichroism Spectroscopy in Combination with *ab Initio* Hartree–Fock Calculations. *Journal of Medicinal Chemistry*, 55(11), 5403-5412. DOI: 10.1021/jm300345z

DTU Library

Technical Information Center of Denmark

General rights

Copyright and moral rights for the publications made accessible in the public portal are retained by the authors and/or other copyright owners and it is a condition of accessing publications that users recognise and abide by the legal requirements associated with these rights.

- Users may download and print one copy of any publication from the public portal for the purpose of private study or research.
- You may not further distribute the material or use it for any profit-making activity or commercial gain
- You may freely distribute the URL identifying the publication in the public portal

If you believe that this document breaches copyright please contact us providing details, and we will remove access to the work immediately and investigate your claim.

Structure–Activity Relationship Study of Selective Excitatory Amino Acid Transporter Subtype 1 (EAAT1) Inhibitor 2-Amino-4-(4-methoxyphenyl)-7-(naphthalen-1-yl)-5-oxo-5,6,7,8-tetrahydro-4*H*-chromene-3-carbonitrile (UCPH-101) and Absolute Configurational Assignment Using Infrared and Vibrational Circular Dichroism Spectroscopy in Combination with *ab Initio* Hartree–Fock Calculations

Tri H. V. Huynh,[†] Irene Shim,[‡] Henrik Bohr,[§] Bjarke Abrahamsen,[†] Birgitte Nielsen,[†] Anders A. Jensen,[†] and Lennart Bunch^{*†}

[†]Department of Drug Design and Pharmacology, Faculty of Health and Medical Sciences, University of Copenhagen, Universitetsparken 2, DK-2100 Copenhagen, Denmark

[‡]Department of Chemistry, Technical University of Denmark, Kemitorvet build. 206, 2800 Kgs. Lyngby, Denmark

[§]Quantum Protein Centre, Department of Physics, Technical University of Denmark, Fysikvej build. 309, 2800 Kgs. Lyngby, Denmark

Supporting Information

ABSTRACT: The excitatory amino acid transporters (EAATs) play essential roles in regulating the synaptic concentration of the neurotransmitter glutamate in the mammalian central nervous system. To date, five subtypes have been identified, named EAAT1–5 in humans, and GLAST, GLT-1, EAAC1, EAAT4, and EAAT5 in rodents, respectively. In this paper, we present the design, synthesis, and pharmacological evaluation of seven 7-*N*-substituted analogues of UCPH-101/102. Analogue **9** inhibited EAAT1 in the micromolar range (IC_{50} value 20 μ M), whereas analogues **8** and **10** were inactive (IC_{50} values >100 μ M). The diastereomeric pairs **11a/11b** and **12a/12b** were separated by HPLC and the absolute configuration assigned by VCD technique in combination with *ab initio* Hartree–Fock calculations. Analogues **11a** (*RS*-isomer) and **12b** (*RR*-isomer) inhibited EAAT1 (IC_{50} values 5.5 and 3.8 μ M, respectively), whereas analogues **11b** (*SS*-isomer) and **12a** (*SR*-isomer) failed to inhibit EAAT1 uptake (IC_{50} values >300 μ M).



inhibited EAAT1 (IC_{50} values 5.5 and 3.8 μ M, respectively), whereas analogues **11b** (*SS*-isomer) and **12a** (*SR*-isomer) failed to inhibit EAAT1 uptake (IC_{50} values >300 μ M).

INTRODUCTION

In the central nervous system (CNS), the excitatory amino acid transporters (EAATs) are responsible for the uptake of the major excitatory neurotransmitter (*S*)-glutamate (Glu) from the synaptic cleft into glial cells and neurons. Thus, the EAATs are key players in the maintenance of synaptic as well as extrasynaptic Glu concentrations below levels of neurotoxicity.¹ To date, five EAAT subtypes have been identified, termed EAAT1–5 in humans, whereas they are termed GLAST, GLT-1, EAAC1, EAAT4, and EAAT5, respectively, in rodents. The five EAAT subtypes exhibit distinct expression patterns in the CNS: while EAAT1–3 (GLAST, GLT-1, and EAAC1, respectively) are expressed throughout the CNS, the EAAT4 subtype is expressed exclusively in Purkinje cells of the cerebellum and EAAT5 only in the retina.² At the cellular level, EAAT1,2 are expressed predominantly in glia cells and

astrocytes, whereas EAAT3,4 are expressed almost exclusively in neurons.³ Finally, EAAT1–3 are high-capacity Glu transporters, while EAAT4,5 are considered to be low-capacity Glu transporters, functioning primarily as Glu-gated chloride ion channels.³ Malfunction of the EAATs has been suggested to be a contributing factor in neurotoxic states and neurodegenerative diseases such as Alzheimer's,⁴ Huntington's,⁵ amyotrophic lateral sclerosis (ALS),⁶ cerebral stroke⁷ and epilepsy,^{1,8,9} as well as in psychiatric disorders like depression¹⁰ and schizophrenia.^{11,12}

We have recently reported the first class of selective EAAT1 inhibitors and a first structure–activity-relationship (SAR) study.^{13,14} The analogues UCPH-101 and UCPH-102 were the

Received: March 13, 2012

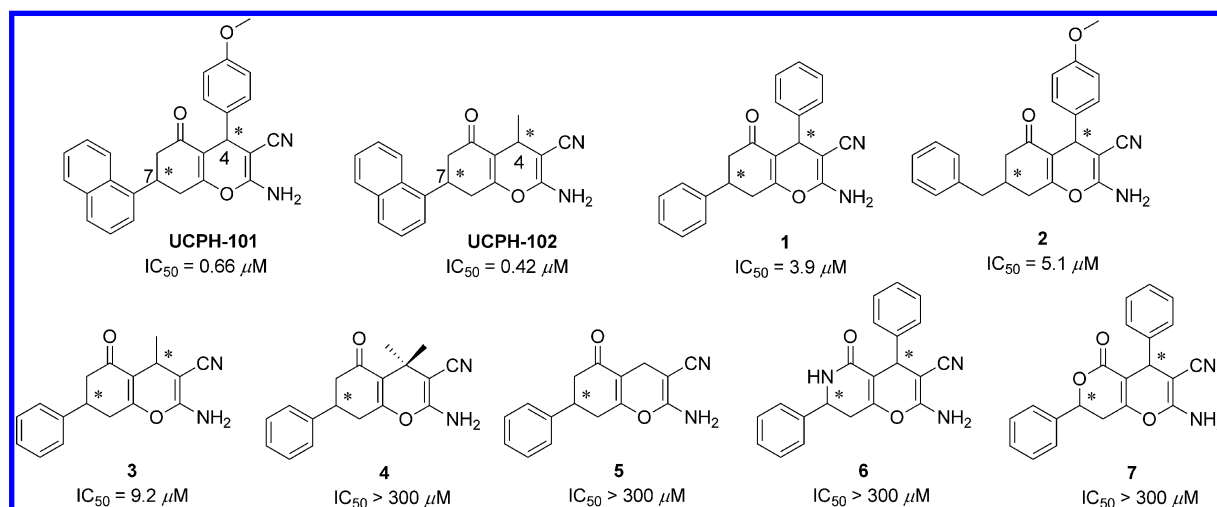


Figure 1. Chemical structures of selective EAAT1 inhibitors UCPH-101 and UCPH-102 together with key analogues from previously reported SAR studies (* indicates stereogenic centers).

most potent inhibitors in the series (IC_{50} values 0.66 and 0.43 μM , respectively) (Figure 1).^{13,14} Comprising two chiral centers, all analogues in the series were synthesized and characterized pharmacologically as a mixture of four stereoisomers (Figure 2), however, the inhibitory activity resides in

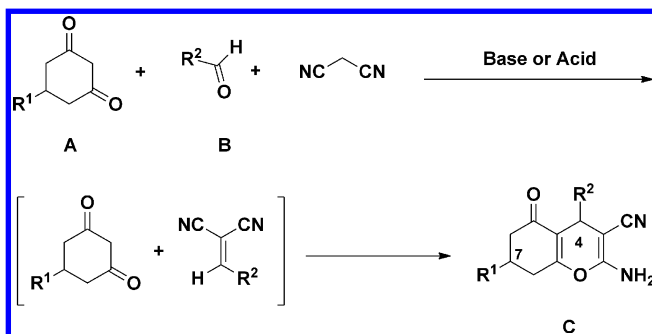


Figure 2. Three component reaction of diketone A, aldehyde B, and malononitrile for the preparation of the 2-amino-5-oxo-5,6,7,8-tetrahydro-4H-chromene-3-carbonitrile parental skeleton C with various substituents R^1 in the 7-position and R^2 in the 4-position.

only two of these.¹³ In this paper, we present the elucidation of the stereochemical configuration in correlation with inhibitory activity for this new class of selective EAAT1 inhibitors.

RESULTS AND DISCUSSION

Design and Synthesis. The synthesis of the UCPH-101/102 compound class (Figure 1) is in general terms carried out by a three-component reaction (Figure 2).¹³ The R^1 substituent in the 7-position of the parental skeleton C originates from diketone A, whereas the R^2 substituent is derived from aldehyde B.

The previously reported SAR study of UCPH-101 and UCPH-102 concluded that the presence of an aromatic ring in the 7-position (R^1) is essential for inhibitory activity and that a 1-naphthyl group (UCPH-101 and UCPH-102) is superior (Figure 1 and Figure 2).^{3,13} On the other hand, the 4-position (R^2) was found to be able to accommodate substituents of various sizes, not being restricted to aromatic moieties (compounds 1–3, Figure 1). Furthermore, two methyl groups or no substituent in the 4-position was observed to result in

complete loss of inhibitory activity at EAAT1 (compounds 4–5, Figure 1). In regard to the stereochemical configuration at the 4 and 7-positions, an in silico study concluded that the stereochemical configuration at C7 (R^1) has little influence on the spatial orientation of the substituent, whereas the substituent at 4-position (R^2) adapts distinct spatial orientation on inverting the stereochemistry (Figure 3). This finding is

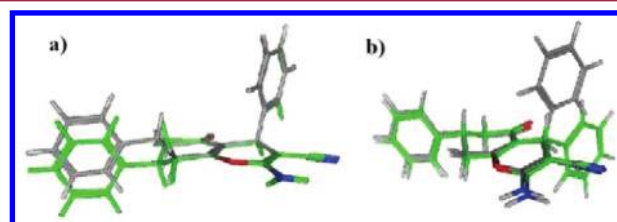


Figure 3. Superimposition of low-energy conformations of 1. (a) Stereochemistry at C4 (R^2) is conserved: *syn*-isomer (green) and *anti*-isomer (gray); (b) stereochemistry at C7 (R^1) is conserved: *syn*-isomer (green) and *anti*-isomer (gray).

intriguing, and together with the fact that 4,4-dimethyl analogue 4 is inactive allowed for the conclusion that the stereochemical configuration at C4 is essential for inhibitory activity.¹³ To elucidate the stereochemical requirements for inhibitory activity, desymmetrization of the diketone fragment by introduction of a heteroatom seemed as an attractive approach. Starting with the enantiopure keto-lactam,^{15,16} a diastereomeric pairs of the final products 6 or 7 would be obtained. Following separation by chromatography, the absolute configuration could be determined by X-ray crystallography. Unfortunately, lactam 6 and lactone 7 were both without inhibitory activity at EAAT1.¹³

To continue the objective, the strategy was modified as to introduce a nitrogen atom in the 7-position (Figure 4). By this tactic, the four stereoisomers is reduced to two, although it is unclear what the consequence of the presence of a basic nitrogen is for EAAT1 inhibitory activity (Figure 4). The 7-N-analogue 8 was designed in accordance with 1, comprising a phenyl group in the 4- and 7-positions. The basicity of the aniline nitrogen functionality is thus limited but also the free rotation of the 7-N-phenyl ring. For analogue 9, the more flexible N-benzyl group was incorporated based on the SAR

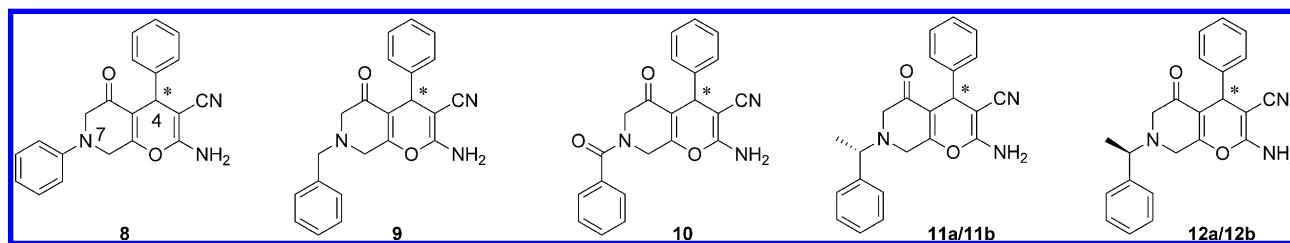


Figure 4. Chemical structures of newly designed 7-*N*-analogues.

observation that a 7-benzyl group is allowed (Figure 2, compound 2). To broaden the SAR study further, analogue 10 was designed comprising an amide functionality in the 7-position. The two pairs of diastereomers, 11a/11b and 12a/12b, comprising an enantiomerically pure substituent in the 7-position (R^1), were designed to resemble benzyl analogue 2 (Figure 2). The diastereomeric mixtures 11a/b and 12a/b were planned to be separated by HPLC and subsequently the absolute stereochemistry assigned by X-ray crystallography or IR/VCD investigations.

The synthesis of the 7-*N*-analogues was to be carried out by the three component reaction already described (Figure 1). Thus the synthesis of aminodiketone D comprising the appropriate *N*-substituent was to be pursued first and subsequently react it with 2-benzylidenemalononitrile (13) to afford the final product, compounds 8–12b (Figure 5).^{3,13}

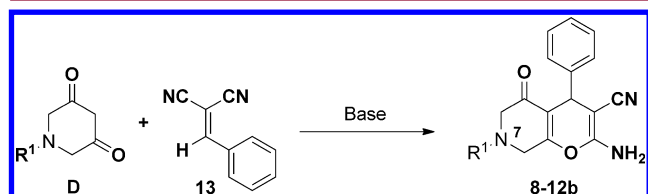


Figure 5. Various diketones D react with 13 to afford 8–12b.

The synthesis of target structure 7-*N*-phenyl 8 commenced with the synthesis of secondary amine 14 by *N*-alkylation of commercially available aniline and ethyl 2-bromoacetate in 46% yield (Scheme 1).¹⁷ Subsequently, *N*-alkylation of 14 with chloroacetone, NaI, and K_2CO_3 in THF afforded tertiary amine 15 in 31% yield.

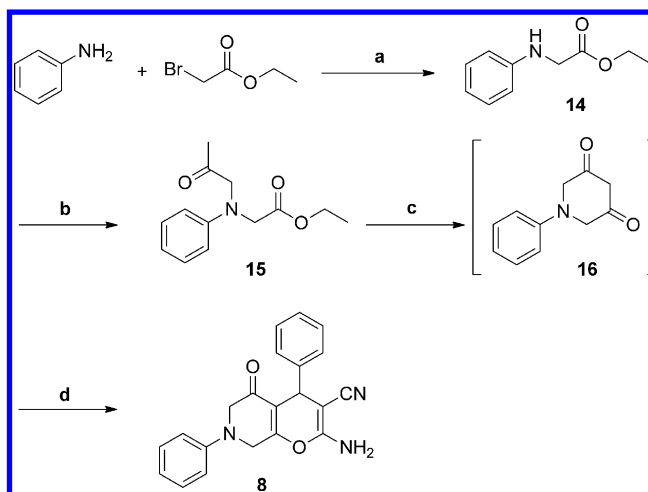
With tertiary amine 15 in hand, reaction with *t*-BuOK in THF afforded diketone 16. Because 16 was found to be unstable on contact with silica,¹⁸ crude 16 was immediately converted to the target compound 7-*N*-phenyl 8 upon reaction with 13¹³ (Scheme 1).

The synthesis of 7-*N*-benzyl 9 (Scheme 2) followed the same strategy as for 8. Diketone 19, also decomposed on silica gel,¹⁸ thus crude 19 was converted directly into 7-*N*-benzyl analogue 9 in 57% yield (Scheme 2).

The synthesis of 7-*N*-benzoyl analogue 10 was first explored by *N*-debenzylation of 9. However, all attempts failed (BzCl, Pd/C and H_2 (g), Pd/C, H_2 (g) and TFA, Pd/C, H_2 (g) and concd HCl) at room temperature and atmospheric pressure were tried.^{19,20} Either full *N*-debenzylation was not achieved or a complex reaction mixture was obtained, including reduction of the two double bonds (observed by NMR).

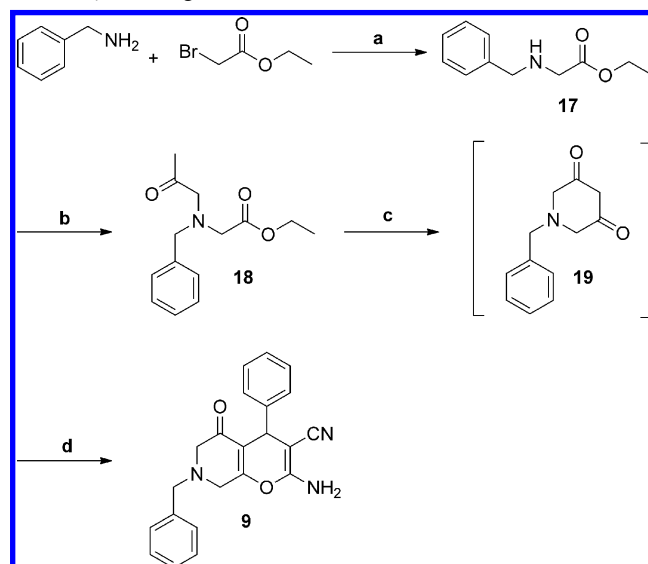
Alternatively, *N*-debenzylation of tertiary amine 18 by hydrogenolysis gave the hydrochloride salt of secondary amine 20 in 97% yield (Scheme 3).²⁰ Subsequently, amine 20 was reacted with benzoyl chloride and Et_3N as base, in THF,

Scheme 1. Synthetic Pathway towards 7-*N*-Phenyl Analogue 8^a



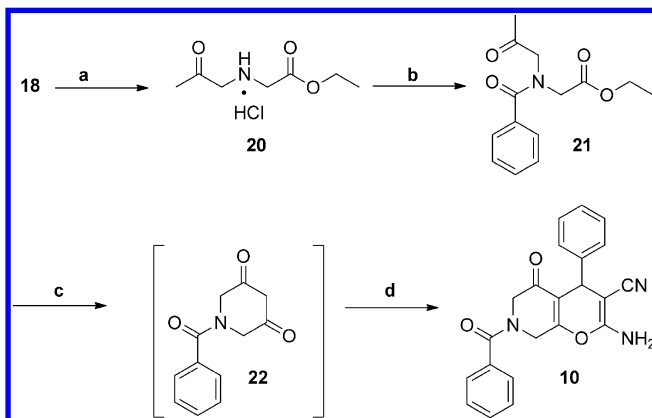
^aReagents and conditions: (a) DIEA, dry acetonitrile, 60 °C, 3 h, 46%; (b) chloroacetone, NaI, K_2CO_3 , dry THF, 60 °C, 3 days, 31%, (c) *t*-BuOK, dry THF, 19 h; (d) 2-benzylidinemalononitrile, piperidine, abs EtOH/ H_2O (3:1), 19 h, 51%.

Scheme 2. Reactions and Conditions for the Synthesis of 7-*N*-Benzyl Analogue 9^a



^aReagents and conditions: (a) dry THF, rt, 3.5 h, 90%; (b) chloroacetone, $NaHCO_3$, abs EtOH, 60 °C, 18 h, 68%; (c) *t*-BuOK, dry THF, 17.5 h; (d) 2-benzylidinemalononitrile, piperidine, abs EtOH/ H_2O (10:1), 24 h, 57%.

Scheme 3. Reagents and Conditions for the Synthesis of 7-*N*-Benzoyl Analogue 10^a

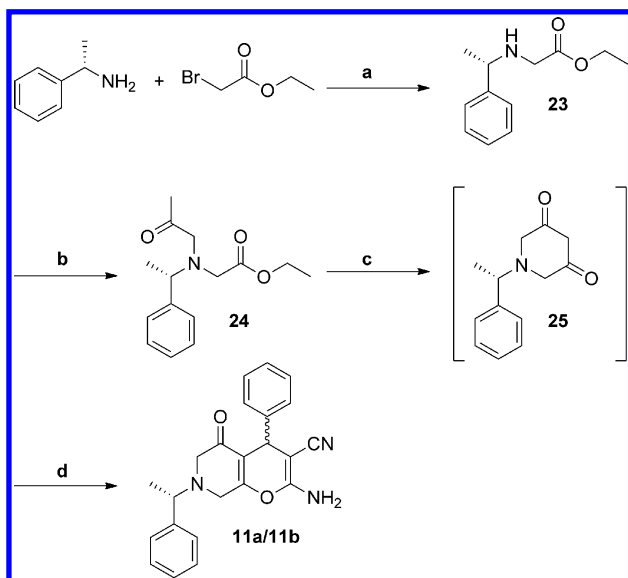


^aReagents and conditions: (a) Pd/C, concd HCl, H₂(g), abs EtOH, 2 h, 97%; (b) Et₃N, benzoyl chloride, dry THF, 14 h, 88%; (c) *t*-BuOK, dry THF, 20 h; (d) 13, piperidine, abs EtOH/H₂O (3:1), 26 h, 55%.

to give amide **21** in 88% yield. Cyclization of amide **21** using *t*-BuOK in THF afforded the unstable diketone **22**, which was immediately converted to the 7-*N*-benzoyl analogue **10** by condensation with **13**¹³ (Scheme 3).

The synthesis of the diastereomeric pairs **11a/11b** commenced with the preparation of amine **23** from alkylation of (*S*)-1-phenylethylamine with ethyl 2-bromoacetate.²¹ A second alkylation with chloroacetone afforded tertiary amine **24**. Basic cyclization of tertiary amine **24** afforded crude diketone **25**, which was condensed with **13**¹³ to give a diastereomeric mixture of **11a/11b** in a 1:1 ratio in overall 41% yield (Scheme 4). Separation of the diastereomeric mixture by chiral HPLC afforded enantiopure **11a** and **11b**. The synthesis of the diastereomeric pair **12a/12b** followed the same strategy as for **11a/11b** but with (*R*)-1-phenylethylamine as starting

Scheme 4. Synthetic Pathway Towards the Diastereomeric Pairs, 11a and 11b^a



^aReagents and conditions: (a) dry THF, rt, 2.5 h, 92%; (b) chloroacetone, NaHCO₃, abs EtOH, 60 °C, 72 h, 21%; (c) *t*-BuOK, dry THF, 2 h; (d) 13, piperidine, abs EtOH/H₂O (10:3), 18 h, 41%.

material. A diastereomeric mixture of **12a/12b** was obtained in a 1:1 ratio in 58% yield, and separation by HPLC gave enantiopure **12a** and **12b**. To assign the stereochemical configuration at C4 of **11a/11b** and **12a/12b**, an X-ray crystallography study seemed attractive but it proved impossible to obtain crystals of **11a/11b** or **12a/12b** of sufficient quality.

Vibrational Circular Dichroism (VCD) and Fast Fourier Transform Infrared (FTIR) Spectroscopy. In combination with ab initio Hartree–Fock (HF) calculations, VCD is a valuable experimental method for the unambiguous assignment of absolute stereochemical configuration of chiral molecules.^{22–28} For reasons of compound quantities, it was decided to undertake **12a** and **12b** for IR/VCD study. The geometries of (*S*)-2-amino-5-oxo-4-phenyl-7-((*R*)-1-phenylethyl)-5,6,7,8-tetrahydro-4*H*-pyrano[2,3-*c*]pyridine-3-carbonitrile (**S1**, Figure 6) and (*R*)-2-amino-5-oxo-4-phenyl-7-((*R*)-1-phenylethyl)-

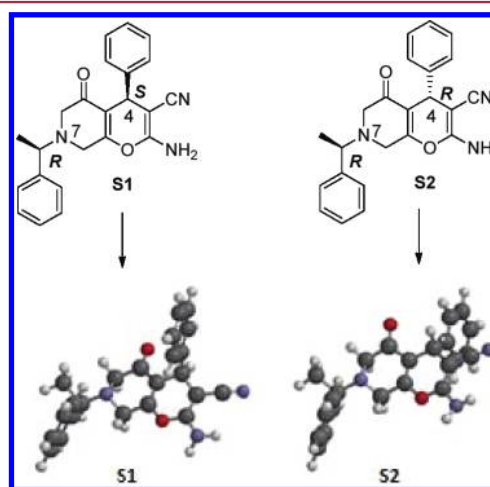


Figure 6. Chemical structures of **S1** and **S2** as well as optimized geometries.

5,6,7,8-tetrahydro-4*H*-pyrano[2,3-*c*]pyridine-3-carbonitrile (**S2**, Figure 6) were optimized (low energy conformation) and used for calculation of IR (see Supporting Information) and VCD spectra (Figure 7).

The calculated IR spectra of **S1** and **S2** are for all importance similar (see Supporting Information). The absorption in the 2850–3000 cm⁻¹ range is due to sp³ C–H stretching, whereas absorption over 3000 cm⁻¹ is from sp³ N–H, sp² C–H, and sp C–H stretching. The absorption peak at 2550 cm⁻¹ originates from the triple bond of CN group, whereas the absorption in the 1450–2000 cm⁻¹ is stretching, bending, and scissoring of alkanes, alkenes, aromatic rings, and ketones. The complexity of absorption in the 500–1450 cm⁻¹ region (fingerprint region) makes it difficult to assign all of the absorption bands for **S1** and **S2** (see Supporting Information). Knowing the IR frequencies, the VCD spectra for **S1** and **S2** could be calculated (Figure 7).

The spectra show high similarity in the 3000–4000 cm⁻¹ region (see Supporting Information), but a clear divergence was observed in the 1450–2000 cm⁻¹ region (Figure 7). For **S1**, positive VCD bands at 1455 cm⁻¹ (C–H and N–H bend) and 1814 cm⁻¹ (C=O stretch) were observed, whereas negative VCD bands were observed for **S2**. Furthermore, at 1552 cm⁻¹ (C=C, C–H, and N–H bend) a negative VCD band for **S1** and a positive VCD band for **S2** were observed.

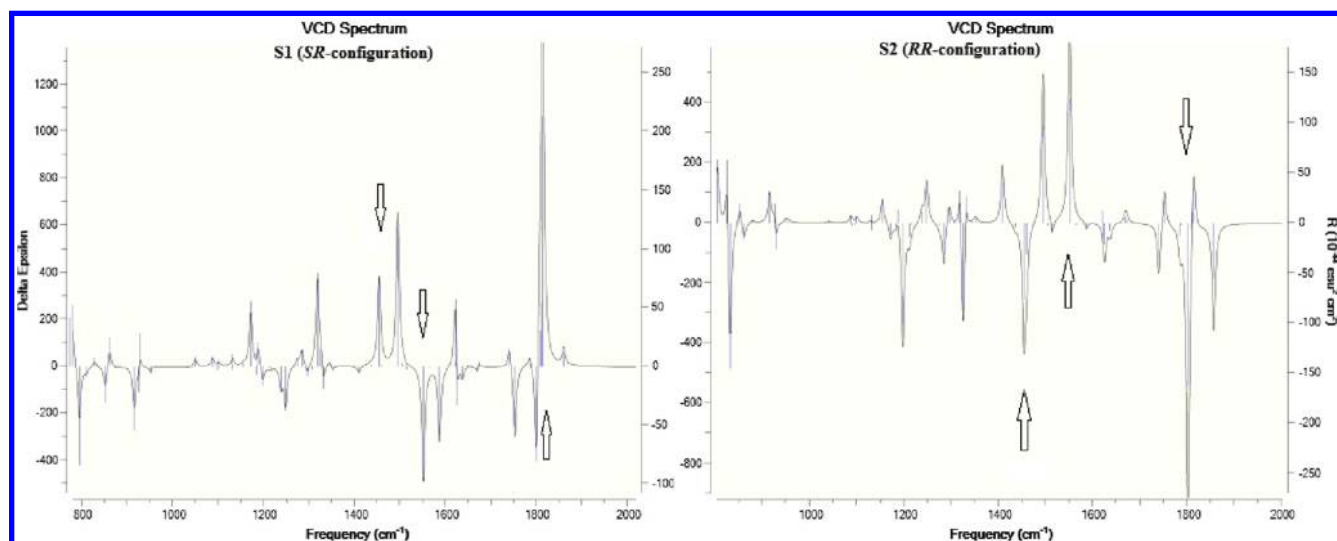


Figure 7. Calculated low-energy conformational VCD of **S1** and **S2** using Gaussian 09. HF method and 6-31G* basis set in gas phase were used. VCD range from 800 to 2000 cm^{-1} , and arrows indicate the three major differences in the VCD bands.

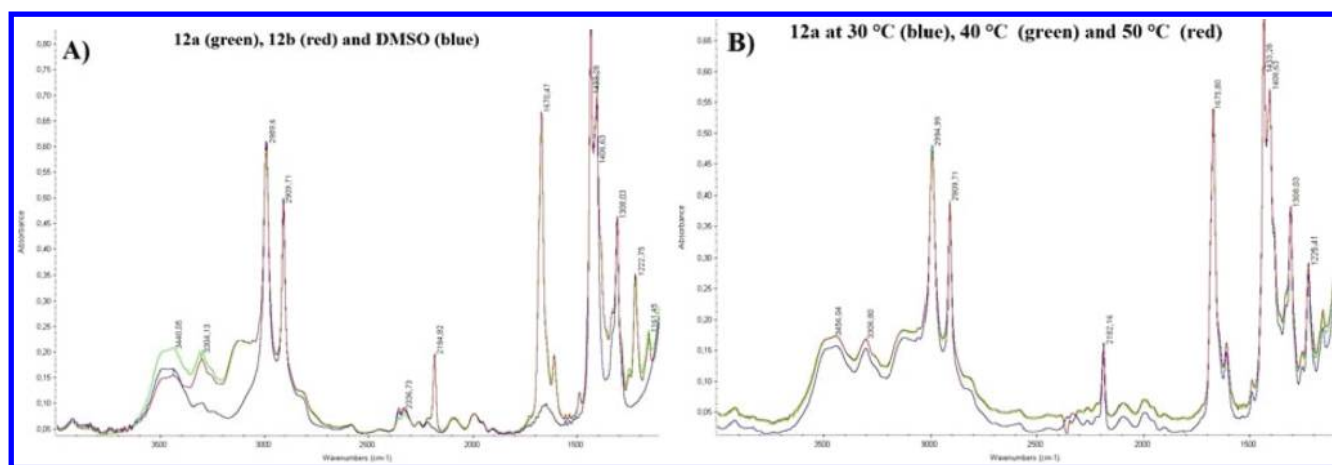


Figure 8. Experimentally determined IR spectra of **12a** and **12b** in DMSO using a FTIR apparatus. (A) IR spectra at rt of **12a** (green) and **12b** (red) at 8 cm^{-1} resolution (20 min) in DMSO (blue) solution (150 mg/mL) using a CaF_2 cell and $6\ \mu\text{m}$ spacer. (B) IR spectra of **12a** at 30 °C (blue), 40 °C (green) and 50 °C (red).

Experimental IR spectra for **12a/12b** were necessary to determine the possibility of measuring the VCD spectra in the desired interval ($1500\text{--}2000\text{ cm}^{-1}$) and to find the optimum IR intensity. The measured IR spectra for **12a/12b**, using a fast transform infrared (FTIR) apparatus are depicted in figure 8.

To determine the optimal IR frequency, several solvents were tried out, of which DMSO gave the best result (Figure 8). Optimal conditions for the $1500\text{--}2000\text{ cm}^{-1}$ region were shown to be a sample concentration of 150 mg/mL in DMSO at 8 cm^{-1} resolution using a calcium fluoride cell and a $6\ \mu\text{m}$ spacer (Figure 8A). Next, an IR temperature-dependent experiment was conducted for **12a** at 30–50 °C, which confirmed that frequencies and absorbance were not critically influenced (Figure 8B). With these conditions in hand, VCD spectra for **12a/12b** were measured using a FTIR apparatus.^{25,29}

Three major differences were observed from the calculated VCD spectra for **S1** and **S2** (Figure 7B). These three frequencies (1455 , 1552 , and 1814 cm^{-1}) have to multiply with 0.8929 to give the experimental frequencies (1299 , 1385 , and 1619 cm^{-1}), which thus can compare with the measured

frequencies. Frequencies 1299 and 1385 cm^{-1} , in the fingerprint region, were not detected because the experimental VCD spectral range was $1500\text{--}2000\text{ cm}^{-1}$. Thus only frequency 1619 cm^{-1} was useful in determining the absolute configurations of **12a** and **12b**.

First, VCD spectrum of DMSO was measured and subtracted from the VCD spectra of **12a/12b**. However, no differences in the VCD spectra of **12a** and **12b** were observed, which was understandable because no IR signal was detected at $1500\text{--}2000\text{ cm}^{-1}$ for DMSO. Fortunately, a positive VCD band was observed for **12a** and a negative VCD band was detected for **12b** at 1614 cm^{-1} for two different concentrations (Figure 9A,B). A minor shift to lower frequency (1604 cm^{-1}) was observed at higher temperatures (Figure 9C,D). This shift in frequency was also detected in the IR spectra (Figure 8).

By comparison of the calculated VCD spectra with the experimentally determined, the stereochemistry of **12a** and **12b** could now be assigned. **S1** and **12a** both displayed a positive VCD band at 1614 and 1619 cm^{-1} , respectively, which unambiguously assigned the *S,R*-configuration to **12a**. Analogue **12b** displayed a negative VCD band at that frequency which

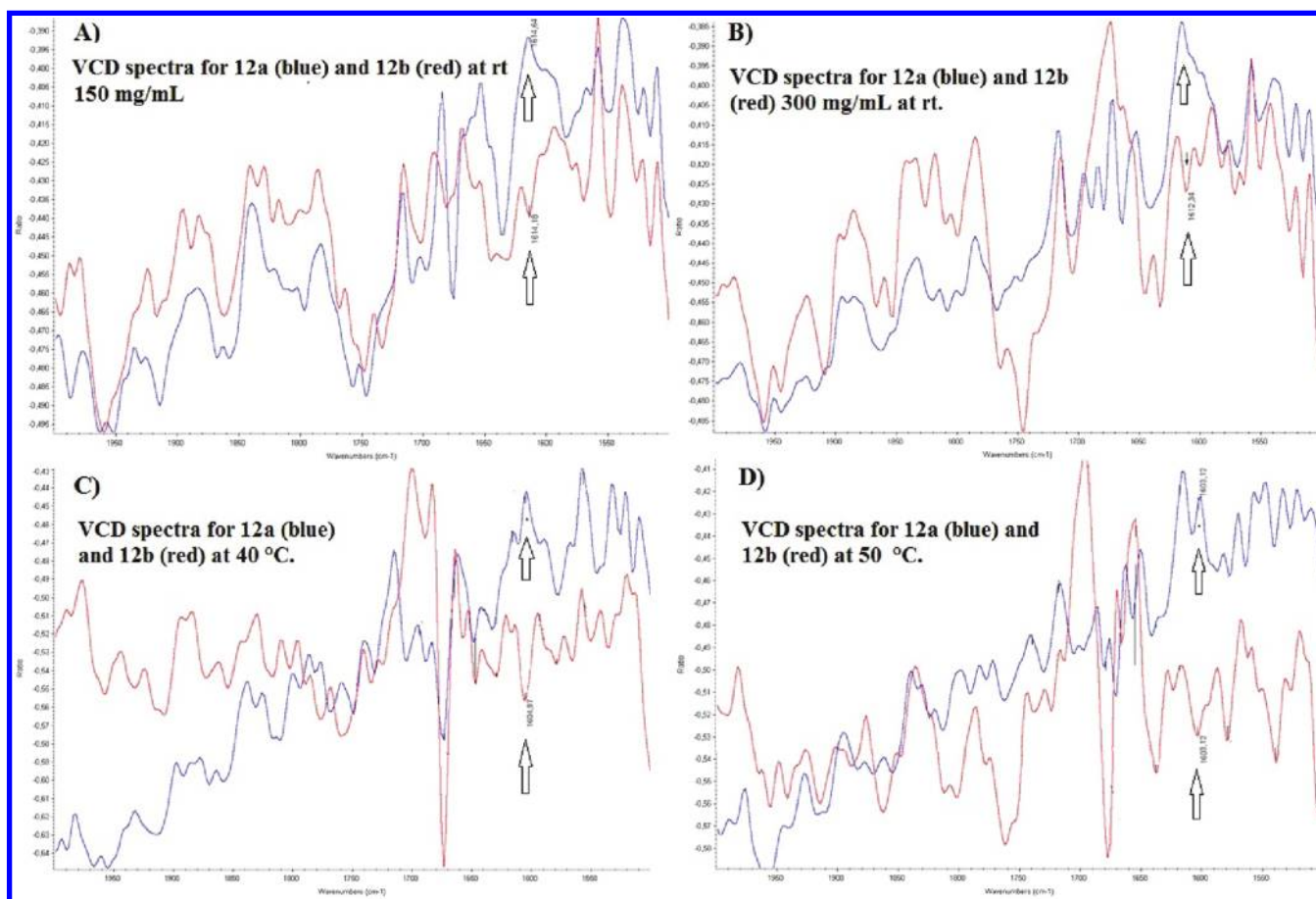


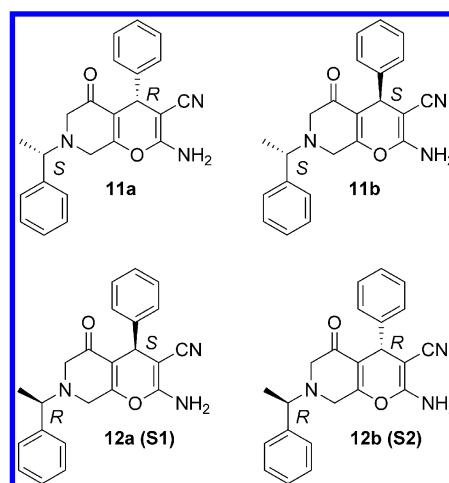
Figure 9. Experimentally determined VCD spectra for 12a and 12b at different concentrations and temperatures. (A) VCD spectra at rt. for 12a (blue) and 12b (red) in DMSO (150 mg/mL). (B) VCD spectra of 12a (blue) and 12b (red) in DMSO (300 mg/mL) at rt. (C) VCD spectra of 12a (blue) and 12b (red) in DMSO (150 mg/mL) at 40 °C. (D) VCD spectra of 12a (blue) and 12b (red) in DMSO (150 mg/mL) at 50 °C. Arrows indicate the major differences in the VCD bands for 12a and 12b.

was in line with **S2** and is thus assigned the *RR*-configuration (Table 1). The absolute configurations of **11a** and **11b** were assigned by comparison of melting points. Given the fact that enantiomers have the same melting point analogues **11a** and **11b** were assigned the *RS*- and *SS*-configuration, respectively (Table 1). Furthermore, comparison of HPLC retention times and NMR data confirmed this assignment.

Pharmacological Characterization. The seven 7-*N*-substituted analogues **8–12b** were characterized pharmacologically at EAAT1–3 in a [³H]-D-Aspartate uptake assay (Table 2).³⁰ 7-*N*-Phenyl analogue **8** displayed no significant inhibitory activity at EAAT1 at a concentration up to 100 μM. In comparison with **1**, it can be concluded that nitrogen atom lonepair delocalization induces a disfavored spatial orientation of the phenyl group.

In comparison with 7-benzyl analogue **2**, the 7-*N*-benzyl analogue **9** retained inhibitory activity at EAAT1 in the medium micromolar range ($IC_{50} = 20 \mu M$). This is explainable because free rotation of the benzyl groups is conserved. Interestingly, the *N*-benzoyl analogue **10** failed to inhibit EAAT1 mediated uptake (Table 2). The enantiopure analogues **11a** and **12b** displayed inhibitory activity at EAAT1 (IC_{50} values 5.5 and 3.8 μM, respectively), while **11b** and **12a** failed to inhibit EAAT1 uptake (Table 2). This confirmed the hypothesis that only one configuration at the 4-position was allowed for (Table 2). None of the synthesized analogues displayed any inhibitory activity at

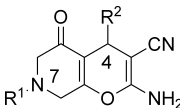
Table 1. Melting Point and the Absolute Configuration of Chiral Analogues 11a–12b



entry	melting point [°C] ^a	R/S isomer
11a	121–123	<i>RS</i>
11b	102–104	<i>SS</i>
12a	121–123	<i>SR</i>
12b	102–104	<i>RR</i>

^aMelting points were measured using a MPA 100 Optimelt automatic melting point system.

Table 2. Pharmacological Characterization of 7-*N*-Substituted Compounds 8–12b as Inhibitors at EAAT1 in a [³H]-D-Aspartate Uptake Assay^a



Compound no	R ¹	R ²	EAAT1 IC ₅₀ [μM]
8			>100 [<4.0]
9			20 [4.79±0.07]
10			>100 [<4.0]
11a			5.5 [5.28±0.09]
11b			>300 [<3.5]
12a			>300 [<3.5]
12b			3.8 [5.43±0.06]

^aData are given as IC₅₀ values in μM with pIC₅₀ ± SEM in brackets. None of the synthesized analogues displayed inhibitory activity at EAAT2 or EAAT3 when applied at the highest possible concentrations (8, 10: IC₅₀ > 100 μM. 9, 11a, 11b, 12a, 12b: IC₅₀ > 300 μM).

the EAAT2,3 subtypes (8, 10: IC₅₀ > 100 μM. 9, 11a, 11b, 12a, 12b: IC₅₀ > 300 μM).

CONCLUSION

In conclusion, seven 7-*N*-substituted analogues 8–12b of EAAT1-selective inhibitors UCPH-101/102 were designed and synthesized. The absolute configuration of enantiopure 11a, 11b, 12a, and 12b was assigned by use of VCD technique in combination with ab initio HF calculations. In an EAAT1 uptake assay, *N*-benzyl analogue 9 displayed inhibitory activity in the midmicromolar range (IC₅₀ = 20 μM), whereas the *N*-phenyl analogue 8 and *N*-benzoyl analogue 10 displayed no EAAT1 inhibitory activity. Enantiopure 11a and 12b inhibited EAAT1 uptake in the low micromolar range (IC₅₀ values 5.5 and 3.8 μM, respectively), whereas their respective diastereomer 11b and 12a was inactive. These results allow for the conclusion that the *R*-configuration in the 4-position is essential for EAAT1 inhibitory activity. This insight may advance future design and synthesis of selective EAAT1 inhibitors.

EXPERIMENTAL SECTION

Chemistry. All reactions involving dry solvents or sensitive agents were performed under a nitrogen atmosphere and glassware was dried prior to use. Solvents were dried according to standard procedures, and reactions were monitored by analytical thin-layer chromatography

(TLC, Merck silica gel 60 F₂₅₄ aluminum sheets). Flash chromatography was carried out using Merck silica gel 60A (35–70 μm). ¹H and ¹³C NMR spectra were recorded on a 300 MHz Varian Mercury 300BB in CDCl₃ using CHCl₃ as internal standard unless otherwise noted. MS spectra were recorded using LC-MS performed using an Agilent 1200 solvent delivery system equipped with an autoinjector coupled to an Agilent 6400 triple quadrupole mass spectrometer equipped with an electrospray ionization source. Gradients of 5% aqueous acetonitrile ≤0.05% formic acid (buffer A) and 95% aqueous acetonitrile +0.043% formic acid (buffer B) were employed. Analytical HPLC was performed using a Dionex UltiMate 3000 pump and photodiode array detector (200 and 210 nm, respectively) installed with an XTerra MS C₁₈ 3.5 μm, 4.6 mm × 150 mm column, using a 5→95% MeCN gradient in H₂O containing 0.1% TFA. Melting points were measured using a MPA 100 OptiMelt automatic melting point system. Optical rotation was measured using a Jasco DIP-370 digital polarimeter, with Na lamp (589 nm). All commercial chemicals were used without further purification. The purity of all tested compounds was determined by elementary analysis and HPLC to be >95%.

2-Amino-5-oxo-4,7-diphenyl-5,6,7,8-tetrahydro-4H-pyrano[2,3-*c*]pyridine-3-carbonitrile (8). A solution of ethyl 2-((2-oxopropyl)(phenyl)amino)acetate (15) (269 mg, 1.14 mmol) in dry THF (4 mL) was added dropwise over 10 min to a suspension of potassium *tert*-butoxide (192 mg, 1.71 mmol) in dry THF (5 mL) at 0 °C under a N₂ atmosphere. The reaction mixture was stirred at rt for 15 h and quenched with satd NaHCO₃ (2 mL). After concentration in vacuo, the crude product was dissolved in EtOH/H₂O (8 mL, 3:1) and 13 (176 mg, 1.14 mmol) and piperidine (45 μL, 456 μmol) were added. The reaction mixture was stirred at rt for 19 h. The reaction mixture was concentrated with silica gel in vacuo and purified by column chromatography on silica gel to afford the title compound as a pale-yellow solid (200 mg, 581 μmol, 51% yield); R_f 0.31 (EtOAc/heptane 1:2). ¹H NMR (300 MHz, DMSO-*d*₆) δ: 7.26–7.08 (m, 9H), 6.98 (d, J = 9.0 Hz, 2H), 6.85 (t, J = 7.6 Hz, 1H), 4.46 (d, J = 17.1 Hz, 1H), 4.27 (s, 1H), 4.15 (d, J = 17.1 Hz, 1H), 4.03 (d, J = 17.4 Hz, 1H), 3.76 (dd, J = 17.1, 1.2 Hz, 1H). ¹³C NMR (75 MHz, DMSO-*d*₆) δ: 193.1, 162.7, 159.0, 149.3, 144.7, 130.0, 129.2, 128.1, 127.6, 120.2, 116.6, 113.4, 59.1, 56.6, 48.6, 35.6; mp 203–205 °C (decomposed). LC-MS (*m/z*) calcd for C₂₁H₁₇N₃O₂ [M + H⁺], 344.1; found, 344.1.

2-Amino-7-benzyl-5-oxo-4-phenyl-5,6,7,8-tetrahydro-4H-pyrano[2,3-*c*]pyridine-3-carbonitrile (9). A solution of ethyl 2-(benzyl(2-oxopropyl)amino)acetate (18) (381 mg, 1.5 mmol) in dry THF (4 mL) was added dropwise over 15 min to a solution of potassium *tert*-butoxide (188 mg, 1.68 mmol) in dry THF (5 mL) at 0 °C under a N₂ atmosphere. The reaction mixture was stirred at rt for 18 h and quenched with satd NaHCO₃ (2 mL). After concentration in vacuo, the crude product was dissolved in abs EtOH (10 mL) and H₂O (1 mL) and 13 (150 mg, 1.1 mmol) and piperidine (20 μL, 216 μmol) were added. The reaction mixture was stirred at rt for 22 h and then concentrated with silica gel in vacuo and purified by column chromatography on silica gel. This afforded the title compound as a pale-yellow solid (222 mg, 619 μmol, 57% yield); R_f 0.20 (EtOAc/heptane 3:5). ¹H NMR (300 MHz, CDCl₃) δ: 7.34–7.18 (m, 10H), 4.53 (s, 2H), 4.42 (s, 1H), 3.65 (d, J = 3.0 Hz 2H), 3.48 (dd, J = 16.8, 0.9 Hz, 1H), 3.32–3.24 (m, 2H), 3.07 (dd, J = 16.2, 2.4 Hz, 1H). ¹³C NMR (75 MHz, CDCl₃) δ: 192.8, 161.2, 157.1, 142.3, 135.8, 129.1, 128.6, 128.5, 127.8, 127.6, 127.3, 118.3, 113.5, 63.6, 61.1, 60.5, 51.3, 34.9; mp 180–182 °C (decomposed). LC-MS (*m/z*) calcd for C₂₂H₁₉N₃O₂ [M + H⁺], 358.1; found, 358.1.

2-Amino-7-benzoyl-5-oxo-4-phenyl-5,6,7,8-tetrahydro-4H-pyrano[2,3-*c*]pyridine-3-carbonitrile (10). A solution of ethyl 2-(*N*-(2-oxopropyl)benzamido)acetate (21) (350 mg, 1.32 mmol) in dry THF (10 mL) was added dropwise to a suspension of potassium *tert*-butoxide (224 mg, 2 mmol) in dry THF (8 mL) at 0 °C under a N₂ atmosphere. The reaction mixture was stirred at rt for 20 h and quenched with satd NH₄Cl (3 mL). After concentration in vacuo, the crude product was dissolved in EtOH/H₂O (12 mL, 3:1) and 13 (113 mg, 0.73 mmol) and piperidine (18 μL, 184 μmol) were added. The reaction mixture was stirred at rt for 26 h, concentrated with silica gel in vacuo, and purified by column chromatography on silica gel. The

title compound was obtained as a pale-yellow solid (148 mg, 399 μmol , 55% yield); R_f 0.32 (EtOAc/heptane 5:1). ^1H NMR (300 MHz, CDCl_3) δ : 7.43–7.21 (m, 10H), 4.97 (s, 3H), 4.18 (s, 1H), 4.25 (d, J = 18.3 Hz, 2H), 3.94 (d, J = 17.7 Hz, 1H). ^{13}C NMR (75 MHz, CDCl_3) δ : 189.6, 160.7, 157.3, 141.9, 133.4, 130.9, 130.8, 128.9, 128.8, 128.7, 127.7, 127.6, 127.3, 127.2, 118.3, 114.1, 62.5, 54.7, 41.5, 35.0; mp 179–181 °C (decomposed). LC-MS (m/z) calcd for $\text{C}_{22}\text{H}_{17}\text{N}_3\text{O}_3$ [$\text{M} + \text{H}^+$], 372.1; found, 372.1.

2-Amino-5-oxo-4-phenyl-7-((S)-1-phenylethyl)-5,6,7,8-tetrahydro-4H-pyrano[2,3-c]pyridine-3-carbonitrile (11a/11b). A suspension of potassium *tert*-butoxide (78 mg, 0.69 mmol) in dry THF (5 mL) was added dropwise to a solution of (S)-ethyl 2-((2-oxopropyl)-(1-phenylethyl)amino)acetate (**24**) (122 mg, 0.46 mmol) in dry THF (8 mL) at 0 °C under a N_2 atmosphere. The reaction mixture was stirred at rt for 2 h and quenched with satd NH_4Cl (2 mL). After concentration in vacuo, the crude product was dissolved in EtOH/ H_2O (6.5 mL, 10:3) and **13** (71 mg, 0.49 mmol) were added. The reaction mixture was stirred at rt for 18 h. After concentration with silica gel in vacuo, the crude product was purified by column chromatography on silica gel. This afforded the title compound as a pale-yellow solid (69 mg, 189 μmol , 41% yield); R_f 0.24 (EtOAc/heptane 1:1). The diastereoisomeric mixture was separated by HPLC using a Chiralpak AD column (*n*-heptane/2-PrOH 80:20) to give **11a** and **11b** (1:1) in 88% yield. Analytical data for **11a** (99.7% de): t_R = 14.6 min (*n*-heptane/2-PrOH 80:20). ^1H NMR (300 MHz, CDCl_3) δ : 7.36–7.19 (m, 10H), 4.50 (s, 2H), 4.41 (s, 1H), 3.54 (q, J = 6.6 Hz, 1H), 3.44 (d, J = 16.5 Hz, 1H), 3.38 (d, J = 15.9 Hz, 1H), 3.18 (d, J = 16.5 Hz, 1H), 2.98 (d, J = 15.9 Hz, 1H), 1.40 (d, J = 6.6 Hz, 3H). ^{13}C NMR (75 MHz, CDCl_3) δ : 193.0, 161.8, 157.2, 142.2, 141.5, 128.7, 128.6, 127.7, 127.6, 127.4, 127.3, 118.4, 113.3, 63.8, 63.5, 58.3, 49.7, 34.8, 19.6; mp 121–123 °C (decomposed). $[\alpha]_D^{25} +10.3^\circ$ (c 0.12, abs EtOH). LC-MS (m/z) calcd for $\text{C}_{23}\text{H}_{21}\text{N}_3\text{O}_2$ [$\text{M} + \text{H}^+$], 372.2; found, 372.2. Analytical data for **11b** (99.7% de): t_R = 12.3 min (*n*-heptane/2-PrOH 80:20). ^1H NMR (300 MHz, CDCl_3) δ : 7.35–7.17 (m, 10H), 4.51 (s, 2H), 4.39 (s, 1H), 3.58 (q, J = 6.6 Hz, 1H), 3.55 (dd, J = 1.5, 16.2 Hz, 1H), 3.28 (dt, J = 2.1, 16.5 Hz, 1H), 3.20 (dd, J = 1.5, 16.2 Hz, 1H), 3.02 (dd, J = 2.1, 16.5 Hz, 1H), 1.41 (d, J = 6.6 Hz, 3H). ^{13}C NMR (75 MHz, CDCl_3) δ : 192.9, 161.7, 157.2, 142.3, 141.2, 128.7, 128.6, 127.7, 127.6, 127.5, 127.3, 118.3, 113.3, 63.7, 63.6, 58.0, 49.7, 34.9, 19.2; mp 102–104 °C (decomposed). $[\alpha]_D^{25} +31.5^\circ$ (c 0.13, abs EtOH). LC-MS (m/z) calcd for $\text{C}_{23}\text{H}_{21}\text{N}_3\text{O}_2$ [$\text{M} + \text{H}^+$], 372.2; found, 372.2.

2-Amino-5-oxo-4-phenyl-7-((R)-1-phenylethyl)-5,6,7,8-tetrahydro-4H-pyrano[2,3-c]pyridine-3-carbonitrile (12a/12b). A suspension of potassium *tert*-butoxide (93 mg, 0.82 mmol) in dry THF (5 mL) was added dropwise to a solution of (R)-ethyl 2-((2-oxopropyl)-(1-phenylethyl)amino)acetate (145 mg, 0.55 mmol) in THF (5 mL) at 0 °C under a N_2 atmosphere. The reaction mixture was stirred at rt for 3 h and quenched with satd NH_4Cl (1 mL). After concentration in vacuo, the crude product was dissolved in EtOH/ H_2O (6 mL, 5:1) and **13** (84 mg, 0.55 mmol) and piperidine (11 μL , 0.20 mmol) were added. The reaction mixture was stirred at rt for 22 h. After concentration with silica gel in vacuo, the crude product was purified by column chromatography on silica gel. This afforded the title compound as a pale-yellow solid (117 mg, 0.32 mmol, 58% yield); R_f 0.33 (EtOAc/heptane 1:1). The diastereoisomeric mixture was separated by HPLC using a Chiralpak AD column (*n*-heptane/2-PrOH 80:20) to give **12a** and **12b** (1:1) in 82% yield. Analytical data for **12a** (99.8% de): t_R = 11.0 min (*n*-heptane/2-PrOH 80:20). ^1H NMR (300 MHz, CDCl_3) δ : 7.36–7.17 (m, 10H), 4.58 (s, 2H), 4.40 (s, 1H), 3.53 (q, J = 6.6 Hz, 1H), 3.43 (d, J = 16.5 Hz, 1H), 3.37 (d, J = 15.9 Hz, 1H), 3.17 (dt, J = 1.5, 16.5 Hz, 1H), 2.98 (dd, J = 2.4, 16.2 Hz, 1H), 1.39 (d, J = 6.6 Hz, 3H). ^{13}C NMR (75 MHz, CDCl_3) δ : 193.0, 161.9, 157.3, 142.3, 141.5, 128.7, 128.6, 127.6, 127.4, 127.3, 118.5, 113.2, 63.8, 63.1, 58.3, 49.7, 34.8, 19.6; mp 121–123 °C (decomposed). $[\alpha]_D^{25} +15.9^\circ$ (c 0.23, abs EtOH). LC-MS (m/z) calcd for $\text{C}_{23}\text{H}_{21}\text{N}_3\text{O}_2$ [$\text{M} + \text{H}^+$], 372.2; found, 372.2. Analytical data for **12b** (99.2% de): t_R = 15.5 min (*n*-heptane/2-PrOH 80:20). ^1H NMR (300 MHz, CDCl_3) δ : 7.35–7.17 (m, 10H), 4.55 (s, 2H), 4.38 (s, 1H), 3.57 (q, J = 6.6 Hz, 1H), 3.54 (dd, J = 1.5, 16.2 Hz, 1H), 3.27 (dt, J =

2.1, 16.5 Hz, 1H), 3.20 (dd, J = 1.5, 16.2 Hz, 1H), 3.01 (dd, J = 2.1, 16.5 Hz, 1H), 1.40 (d, J = 6.6 Hz, 3H). ^{13}C NMR (75 MHz, CDCl_3) δ : 193.0, 161.8, 157.2, 142.3, 141.2, 128.7, 128.6, 127.7, 127.6, 127.4, 127.3, 118.4, 113.3, 63.8, 63.6, 58.0, 49.7, 34.9, 19.3; mp 102–104 °C (decomposed). $[\alpha]_D^{25} -34.5^\circ$ (c 0.23, abs EtOH). LC-MS (m/z) calcd for $\text{C}_{23}\text{H}_{21}\text{N}_3\text{O}_2$ [$\text{M} + \text{H}^+$], 372.2; found, 372.2.

Ethyl 2-(Phenylamino)acetate (14). Ethyl bromoacetate (2.43 mL, 22 mmol) was added dropwise over 2 h to a stirred solution of aniline (2 mL, 22 mmol) and *N,N*-diisopropylethylamine (8 mL, 46 mmol) in acetonitrile (20 mL) at 60 °C. The reaction mixture was stirred for an additional 3 h at 60 °C and then concentrated to dryness. Addition of H_2O (5 mL) to the residue and the solid was filtered and washed with H_2O several times. Recrystallization from toluene afforded the title compound as a beige solid (1.83 g, 10.1 mmol, 46% yield). ^1H NMR (300 MHz, CDCl_3) δ : 7.23–7.13 (m, 2H), 6.74 (t, J = 7.2, 1H), 6.59 (dd, J = 7.8, 0.9 Hz, 2H), 4.23 (q, J = 7.2 Hz, 2H), 3.88 (s, 2H), 1.29 (t, J = 7.2 Hz, 3H). ^{13}C NMR (75 MHz, CDCl_3) δ : 171.1, 147.0, 129.2, 118.1, 112.9, 61.3, 45.8, 14.2; mp 55–57 °C (decomposed). LC-MS (m/z) calcd for $\text{C}_{10}\text{H}_{13}\text{NO}_2$ [$\text{M} + \text{H}^+$], 180.1; found, 180.1.

Ethyl 2-((2-Oxopropyl)(phenylamino)acetate (15). Ethyl 2-(phenylamino)acetate (**14**) (1 g, 5.6 mmol) and K_2CO_3 (2.31 g, 16.7 mmol) were stirred in dry THF (30 mL) at rt under a N_2 atmosphere. A solution of chloroacetone (489 μL , 6.14 mmol) in dry THF (4 mL) was added dropwise to the reaction mixture and stirred for 30 min. Sodium iodide (920 mg, 6.14 mmol) was added, and the reaction mixture was stirred at 60 °C for 3 days. The crude reaction was quenched with H_2O (10 mL) and extracted with EtOAc (3 \times 30 mL), and the combined organic phases were washed with H_2O (1 \times 30 mL) and brine (1 \times 20 mL). The organic phase was dried over MgSO_4 . After concentration in vacuo, the crude product was purified by column chromatography on silica gel. This afforded the title compound as a pale-yellow oil (448 mg, 1.73 mmol, 31% yield); R_f 0.25 (EtOAc/heptane 1:2). ^1H NMR (300 MHz, CDCl_3) δ : 7.24–7.16 (m, 2H), 6.76 (dt, J = 7.2, 0.6 Hz, 1H), 6.53 (dd, J = 7.8, 0.9 Hz, 2H), 4.19 (q, J = 7.2 Hz, 2H), 4.12 (s, 2H), 4.09 (s, 2H), 2.19 (s, 3H), 1.27 (t, J = 7.2 Hz, 3H). ^{13}C NMR (75 MHz, CDCl_3) δ : 207.7, 170.8, 147.7, 129.3, 118.3, 112.4, 62.3, 61.1, 53.8, 27.0, 14.2. LC-MS (m/z) calcd for $\text{C}_{13}\text{H}_{17}\text{NO}_3$ [$\text{M} + \text{H}^+$], 236.1; found, 236.1.

Ethyl 2-(Benzylamino)acetate (17). A solution of ethyl bromoacetate (924 μL , 8 mmol) in dry THF (4 mL) was added dropwise over 10 min to a cooled solution of benzylamine (2 mL, 18 mmol) in dry THF (20 mL) at 0 °C under a N_2 atmosphere. The reaction mixture was stirred for 3.5 h at rt, where after it was concentrated and resuspended in diethyl ether. The white solid was filtered off. The crude was concentrated and purified by column chromatography on silica gel. This afforded the title compound as a pale-yellow oil (1.45 g, 7.50 mmol, 90% yield); R_f 0.26 (EtOAc/heptane 1:1). ^1H NMR (300 MHz, CDCl_3) δ : 7.34–7.20 (m, 5H), 4.18 (q, J = 7.2 Hz, 2H), 3.80 (s, 2H), 3.40 (s, 2H), 1.89 (s, 1H), 1.27 (t, J = 7.2 Hz, 3H); ^{13}C NMR (75 MHz, CDCl_3) δ : 172.3, 139.5, 128.4, 128.2, 127.1, 60.7, 53.2, 50.1, 14.2. LC-MS (m/z) calcd for $\text{C}_{11}\text{H}_{15}\text{NO}_2$ [$\text{M} + \text{H}^+$], 194.1; found, 194.1.

Ethyl 2-(Benzyl(2-oxopropyl)amino)acetate (18). Ethyl 2-(benzylamino)acetate (**17**) (165 mg, 853 μmol) and NaHCO_3 (72 mg, 853 μmol) were stirred in abs EtOH (3 mL) at 60 °C under a N_2 atmosphere. A solution of chloroacetone (68 μL , 853 μmol) in abs EtOH (1 mL) was added dropwise to the reaction mixture and stirred for 18 h. The crude reaction was quenched with H_2O (5 mL) and extracted with EtOAc (3 \times 10 mL), and the combined organic phases were washed with H_2O (1 \times 10 mL) and brine (1 \times 10 mL). The organic phase was dried over MgSO_4 . After concentration in vacuo, the crude product was purified by column chromatography on silica gel to afford the title compound as a pale-yellow oil (137 mg, 580 μmol , 68% yield); R_f 0.51 (EtOAc/heptane 1:1). ^1H NMR (300 MHz, CDCl_3) δ : 7.34–7.20 (m, 5H), 4.15 (q, J = 6.9 Hz, 2H), 3.83 (s, 2H), 3.52 (s, 2H), 3.45 (s, 2H), 1.26 (t, J = 6.9 Hz, 3H). ^{13}C NMR (75 MHz, CDCl_3) δ : 207.8, 171.0, 138.1, 128.9, 128.4, 127.4, 63.1, 60.4, 58.4, 54.3, 27.5, 14.2. LC-MS (m/z) calcd for $\text{C}_{14}\text{H}_{19}\text{NO}_3$ [$\text{M} + \text{H}^+$], 250.1; found, 250.1.

Ethyl 2-(2-Oxopropylamino)acetate (20). Ethyl 2-(benzyl(2-oxopropyl)amino)acetate (**18**) (1.19 g, 4.76 mmol) was stirred in abs EtOH (20 mL) at rt. under and a N₂ atmosphere. Conc'd HCl (1 mL) and Pd/C (118 mg, 476 μmol) were added, and the reaction mixture was purged with H₂ (g) for 2 h. The black solid material was filtered through Celite, and the residue was washed several times with abs EtOH. The filtrate was concentrated to afford the title compound as a beige solid (900 mg, 4.62 mmol, 97% yield). ¹H NMR (300 MHz, MeOH-*d*₄) δ: 4.30 (q, *J* = 6.9 Hz, 2H), 4.19 (s, 2H), 3.96 (s, 2H), 2.24 (s, 3H), 1.32 (t, *J* = 6.9 Hz, 3H). ¹³C NMR (75 MHz, MeOH-*d*₄) δ: 200.2, 166.6, 62.7, 54.8, 46.9, 26.2, 13.4; mp 132–134 °C (decomposed). LC-MS (*m/z*) calcd for C₇H₁₃NO₃ [M + H⁺], 160.1; found, 160.1.

Ethyl 2-(*N*-(2-Oxopropyl)benzamido)acetate (21). Ethyl 2-(2-oxopropylamino)acetate (**20**) (300 mg, 1.53 mmol) was stirred in dry THF (20 mL) at 0 °C under a N₂ atmosphere. A solution of Et₃N (446 μL, 3.22 mmol) in dry THF (2 mL) was added dropwise and stirred for an additional 5 min. A solution of benzoyl chloride (196 μL, 1.69 mmol) in dry THF (1 mL) was added dropwise, and the reaction mixture was stirred at rt for 14 h. The crude reaction was quenched with H₂O (10 mL) and extracted with EtOAc (3 × 30 mL), and the combined organic phases were washed with H₂O (1 × 20 mL) and brine (1 × 20 mL). The organic phase was dried over MgSO₄ and concentrated in vacuo. The crude product was purified by column chromatography on silica gel to afford the title compound as a pale-yellow oil (354 mg, 1.35 mmol, 88% yield); *R*_f 0.29 (EtOAc/heptane 2:1). ¹H NMR (300 MHz, DMSO-*d*₆) δ: 7.43–7.18 (m, 5H, minor and m, 5H, major), 4.30 (s, 2H, minor), 4.22 (s, 2H, major), 4.13–4.04 (m, 2H, minor and m, 2H, major), 4.09 (s, 2H, minor), 3.99 (s, 2H, major), 2.12 (s, 3H, minor), 1.94 (s, 3H, major), 1.21 (t, *J* = 6.0 Hz, 3H, minor), 1.13 (t, *J* = 6.0 Hz, 3H, major). ¹³C NMR (75 MHz, CDCl₃, M = major conformer, m = minor conformer) δ: 202.9 (M and m), 172.2 (M and m), 169.3 (M and m), 134.9 (m), 134.7 (M), 130.2 (M and m), 128.6 (M and m), 126.8 (M), 126.6 (m), 61.6 (M), 61.3 (m), 59.6 (m), 55.6 (M), 51.8 (M), 47.4 (m), 27.4 (M), 27.0 (m), 14.1 (M and m). LC-MS (*m/z*) calcd for C₁₄H₁₇NO₄ [M + H⁺], 264.1; found, 264.1.

(*S*)-Ethyl 2-(1-Phenylethylamino)acetate (23). A solution of ethyl bromoacetate (1 mL, 9 mmol) in dry THF (4 mL) was added dropwise over 10 min to a cooled solution of (*S*)-1-phenylethylamine (2.41 mL, 19 mmol) in dry THF (25 mL) at 0 °C under a N₂ atmosphere. The reaction mixture was stirred for 2.5 h at rt. After concentration in vacuo, the crude product was purified by column chromatography on silica gel. This afforded the title compound as a colorless oil (1.71 g, 8.3 mmol, 92% yield); *R*_f 0.49 (EtOAc/heptane 2:1). ¹H NMR (300 MHz, CDCl₃) δ: 7.30–7.19 (m, 5H), 4.14 (q, *J* = 6.9 Hz, 2H), 3.78 (q, *J* = 6.9 Hz, 1H), 3.24 (AB system, ²*J* = 3.3 Hz, 2H), 1.92 (s, 1H), 1.38 (d, *J* = 6.9 Hz, 3H), 1.23 (t, *J* = 6.9 Hz, 3H). ¹³C NMR (75 MHz, CDCl₃) δ: 172.9, 145.0, 128.9, 127.5, 127.1, 61.1, 58.1, 49.3, 24.7, 14.6. LC-MS (*m/z*) calcd for C₁₂H₁₇NO₂ [M + H⁺], 208.1; found, 208.1.

(*S*)-Ethyl 2-((2-Oxopropyl)(1-phenylethyl)amino)acetate (24). (*S*)-Ethyl-2-(1-phenylethylamino)-acetate (**23**) (1.59 g, 7.67 mmol) and NaHCO₃ (773 mg, 9.21 mmol) were stirred in abs EtOH (25 mL) at 60 °C under a N₂ atmosphere. A solution of chloroacetone (733 μL, 9.21 mmol) in abs EtOH (4 mL) was added dropwise to the reaction mixture and stirred for 3 days. The crude reaction was quenched with H₂O (10 mL) and extracted with EtOAc (3 × 50 mL), and the combined organic phases were washed with H₂O (1 × 50 mL) and brine (1 × 40 mL). The organic phase was dried over MgSO₄. After concentration in vacuo, the crude product was purified by column chromatography on silica gel. This afforded the title compound as a pale-yellow oil (432 mg, 1.61 mmol, 21% yield); *R*_f 0.13 (100% dichloromethane). ¹H NMR (300 MHz, CDCl₃) δ: 7.40–7.22 (m, 5H), 4.17–4.08 (m, 3H), 3.57 (d, *J* = 5.4 Hz, 1H), 3.50 (d, *J* = 5.4 Hz, 1H), 3.43 (d, *J* = 4.2 Hz, 1H), 3.38 (d, *J* = 4.2 Hz, 1H), 2.11 (s, 3H), 1.34 (d, *J* = 6.9 Hz, 3H), 1.25 (t, *J* = 6.9 Hz, 3H). ¹³C NMR (75 MHz, CDCl₃) δ: 208.8, 171.6, 143.9, 128.4, 127.4, 127.3, 61.6, 60.9, 60.4, 52.4, 27.5, 19.8. LC-MS (*m/z*) calcd for C₁₅H₂₁NO₃ [M + H⁺], 264.1; found, 264.1.

HPLC. Analytical HPLC for determination of the diastereomeric excess (de) was performed using a Chiralpak AD column (4.6 mm × 250 mm) equipped with a Chiralpak AD guard column (4 mm × 10 mm) (Daicel) and eluted at 1.0 mL/min with *n*-heptane/2-PrOH (80:20). The column was connected to a Dionex Ultimate 3000 pump, a TSP AS-3000 autosample and a Dionex Ultimate 3000 photodiode array detector. For HPLC control, data collection and data handling, Chromleon software v. 6.80 was used.

Preparative HPLC. Separation of the diastereomeric mixtures was achieved using a Chiralpak AD column (20 mm × 250 mm) and flow rate 6 mL/min with *n*-heptane/2-PrOH (80:20). Sample concentration was 6 mg/mL and injection volume was 2 mL.

IR and VCD. The IR was measured using a fast transform infrared (FTIR) apparatus. VCD spectra were measured using a FTIR apparatus with interferometers and with an IR source operating at Phi-M 400 Hz. A Nicolet Nexus 870 FT-IR spectrometer with the PEM module from Thermo Electron Corporation that has a wide spectral range from 200 to 7000 cm⁻¹ was used. A sample concentration of 150 mg/mL in DMSO at 8 cm⁻¹ resolution using a calcium fluoride (CaF₂) cell and a 6 μm spacer gave an absorbance at 0.7. Calculated VCD frequencies using HF and 6-31G* basis set come out uniformly higher than experimental frequencies. Thus, a scaling factor of 0.8929 for harmonic vibrational frequencies is proposed as being appropriate for predictive purposes.^{31–35}

In Silico Study. The modeling study was performed using the software package MOE (Molecular Operating Environment, Chemical Computing Group, 2010) using the built-in mmff94x forcefield and the GB/SA continuum solvent model. General procedure: The compound of interest was submitted to a stochastic conformational search (standard setup) to determine its low-energy conformation. Superimposition of selected low-energy conformations was done using the built-in function by fitting the three atoms amino groups and the C^{1'}-carbons of the phenyl rings.

Pharmacology. Cell culture of the EAAT1,2,3-HEK293 cell lines and the [³H]-D-Aspartate uptake assay were performed essentially as previously described.³⁰ The experimental procedures are described in detail in Supporting Information.

■ ASSOCIATED CONTENT

📄 Supporting Information

IR and VCD values in table format for **S1** and **S2**, as well as pharmacology experimental procedures. This material is available free of charge via the Internet at <http://pubs.acs.org>.

■ AUTHOR INFORMATION

✉ Corresponding Author

*Phone: +45 35336244. Fax: +45 35336041. E-mail: lebu@farma.ku.dk.

Notes

The authors declare no competing financial interest.

■ ACKNOWLEDGMENTS

We thank Postdoc Karin Stibius Jensen, Quantum Protein Centre, Department of Physics, Technical University of Denmark, for the technical assistance with the VCD spectrometer. We express our gratitude to the Lundbeck Foundation, the Novo Nordisk Foundation, the Augustinus Foundation, the Danish Medical Council, and the Carlsberg Foundation for financial support.

■ ABBREVIATIONS USED

ALS, amyotrophic lateral sclerosis; CNS, central nervous system; EAAC1, excitatory amino acid carrier subtype 1; EAAT(s), excitatory amino acid transporter(s); FTIR, Fast transform infrared; GLAST, glutamate aspartate transporter; GLT-1, glutamate transporter subtype 1; HF, Hartree–Fock;

HPLC, high-performance liquid chromatography; SAR, structure–activity relationship; VCD, vibrational circular dichroism

REFERENCES

- (1) Beart, P. M.; O’Shea, R. D. Transporters for L-glutamate: an update on their molecular pharmacology and pathological involvement. *Br. J. Pharmacol.* **2007**, *150*, 5–17.
- (2) Foster, A. C.; Kemp, J. A. Glutamate- and GABA-based CNS therapeutics. *Curr. Opin. Pharmacol.* **2006**, *6*, 7–17.
- (3) Bunch, L.; Erichsen, M. N.; Jensen, A. A. Excitatory amino acid transporters as potential drug targets. *Expert Opin. Ther. Targets* **2009**, *13*, 719–731.
- (4) Lee, S. G.; Su, Z. Z.; Emdad, L.; Gupta, P.; Sarkar, D.; Borjabad, A.; Volsky, D. J.; Fisher, P. B. Mechanism of ceftriaxone induction of excitatory amino acid transporter-2 expression and glutamate uptake in primary human astrocytes. *J. Biol. Chem.* **2008**, *283*, 13116–13123.
- (5) Estrada Sanchez, A. M.; Mejia-Toiber, J.; Massieu, L. Excitotoxic neuronal death and the pathogenesis of Huntington’s disease. *Arch. Med. Res.* **2008**, *39*, 265–276.
- (6) Corona, J. C.; Tovar-y-Romo, L. B.; Tapia, R. Glutamate excitotoxicity and therapeutic targets for amyotrophic lateral sclerosis. *Expert Opin. Ther. Targets* **2007**, *11*, 1415–1428.
- (7) Muir, K. W. Glutamate-based therapeutic approaches: clinical trials with NMDA antagonists. *Curr. Opin. Pharmacol.* **2006**, *6*, 53–60.
- (8) Sheldon, A. L.; Robinson, M. B. The role of glutamate transporters in neurodegenerative diseases and potential opportunities for intervention. *Neurochem. Int.* **2007**, *51*, 333–355.
- (9) Alexander, G. M.; Godwin, D. W. Metabotropic glutamate receptors as a strategic target for the treatment of epilepsy. *Epilepsy Res.* **2006**, *71*, 1–22.
- (10) Sanacora, G.; Treccani, G.; Popoli, M. Towards a glutamate hypothesis of depression: an emerging frontier of neuropsychopharmacology for mood disorders. *Neuropharmacology* **2012**, *62*, 63–77.
- (11) Karlsson, R. M.; Tanaka, K.; Heilig, M.; Holmes, A. Loss of glial glutamate and aspartate transporter (excitatory amino acid transporter 1) causes locomotor hyperactivity and exaggerated responses to psychotomimetics: rescue by haloperidol and metabotropic glutamate 2/3 agonist. *Biol. Psychiatry* **2008**, *64*, 810–814.
- (12) Karlsson, R. M.; Tanaka, K.; Saksida, L. M.; Bussey, T. J.; Heilig, M.; Holmes, A. Assessment of glutamate transporter GLAST (EAAT1)-deficient mice for phenotypes relevant to the negative and executive/cognitive symptoms of schizophrenia. *Neuropsychopharmacology* **2009**, *34*, 1578–89.
- (13) Erichsen, M. N.; Huynh, T. H.; Abrahamsen, B.; Bastlund, J. F.; Bundgaard, C.; Monrad, O.; Bekker-Jensen, A.; Nielsen, C. W.; Frydenvang, K.; Jensen, A. A.; Bunch, L. Structure–activity relationship study of first selective inhibitor of excitatory amino acid transporter subtype 1: 2-Amino-4-(4-methoxyphenyl)-7-(naphthalen-1-yl)-5-oxo-5,6,7,8-tetrahydro-4H-chromene-3-carbonitrile (UCPH-101). *J. Med. Chem.* **2010**, *53*, 7180–7191.
- (14) Jensen, A. A.; Erichsen, M. N.; Nielsen, C. W.; Stensbol, T. B.; Kehler, J.; Bunch, L. Discovery of the first selective inhibitor of excitatory amino acid transporter subtype 1. *J. Med. Chem.* **2009**, *52*, 912–915.
- (15) Kawecki, R. Addition of dienolates to sulfinimines. Stereo-selective synthesis of dihydropyridones. *Tetrahedron* **2001**, *57*, 8385–8390.
- (16) Davis, F. A.; Fang, T. N.; Chao, B.; Burns, D. M. Asymmetric synthesis of the four stereoisomers of 4-hydroxypipericolic acid. *Synthesis* **2000**, 2106–2112.
- (17) Kotake, Y.; Okauchi, T.; Iijima, A.; Yoshimatsu, K.; Nomura, H. Novel 6–5 fused ring heterocycle antifolates with potent antitumor activity: bridge modifications and heterocyclic benzoyl isomers of 2,4-diamino-6,7-dihydro-5H-cyclopenta[*d*]pyrimidine antifolate. *Chem. Pharm. Bull.* **1995**, *43*, 829–841.
- (18) Olofsson, B.; Bogar, K.; Fransson, A. B.; Backvall, J. E. Divergent asymmetric synthesis of 3,5-disubstituted piperidines. *J. Org. Chem.* **2006**, *71*, 8256–8260.
- (19) Muller, D.; Zeltser, I.; Bitan, G.; Gilon, C. Building Units for N-Backbone Cyclic Peptides. 3. Synthesis of Protected N(alpha)-(omega-Aminoalkyl)amino Acids and N(alpha)-(omega-Carboxyalkyl)amino Acids. *J. Org. Chem.* **1997**, *62*, 411–416.
- (20) Clinch, K.; Evans, G. B.; Frohlich, R. F.; Furneaux, R. H.; Kelly, P. M.; Legentil, L.; Murkin, A. S.; Li, L.; Schramm, V. L.; Tyler, P. C.; Woolhouse, A. D. Third-generation immucillins: syntheses and bioactivities of acyclic immucillin inhibitors of human purine nucleoside phosphorylase. *J. Med. Chem.* **2009**, *52*, 1126–1143.
- (21) Porzi, G.; Sandri, S. Enantioselective Synthesis of (R)- and (S)- α -Amino Acids Using (6S)- and (6R)-6-Methyl-morpholine-2,5-dione Derivatives. *Tetrahedron: Asymmetry* **1996**, *7*, 189–196.
- (22) Monde, K.; Taniguchi, T.; Miura, N.; Vairappan, C. S.; Suzuki, M. Absolute configurations of endoperoxides determined by vibrational circular dichroism (VCD). *Tetrahedron Lett.* **2006**, *47*, 4389–4392.
- (23) Devlin, F. J.; Stephens, P. J.; Osterle, C.; Wiberg, K. B.; Cheeseman, J. R.; Frisch, M. J. Configurational and conformational analysis of chiral molecules using IR and VCD spectroscopies: spiropentylcarboxylic acid methyl ester and spiropentyl acetate. *J. Org. Chem.* **2002**, *67*, 8090–8096.
- (24) Bringmann, G.; Busemann, S. Quantumchemical Calculation of CD Spectra: The Absolute Configuration of Palmarumycins CP3 and C2. *Tetrahedron* **1997**, *53*, 1655–1664.
- (25) Ma, S.; Freedman, T. B.; Dukor, R. K.; Nafie, L. A. Near-infrared and mid-infrared Fourier transform vibrational circular dichroism of proteins in aqueous solution. *Appl. Spectrosc.* **2010**, *64*, 615–626.
- (26) Minick, D. J.; Copley, R. C.; Szewczyk, J. R.; Rutkowske, R. D.; Miller, L. A. An investigation of the absolute configuration of the potent histamine H3 receptor antagonist GT-2331 using vibrational circular dichroism. *Chirality* **2007**, *19*, 731–740.
- (27) Shin-ya, K.; Sugeta, H.; Shin, S.; Hamada, Y.; Katsumoto, Y.; Ohno, K. Absolute configuration and conformation analysis of 1-phenylethanol by matrix-isolation infrared and vibrational circular dichroism spectroscopy combined with density functional theory calculation. *J. Phys. Chem. A* **2007**, *111*, 8598–8605.
- (28) Munoz, M. A.; Munoz, O.; Joseph-Nathan, P. Absolute configuration of natural diastereoisomers of β -hydroxyhyoscyamine by vibrational circular dichroism. *J. Nat. Prod.* **2006**, *69*, 1335–1340.
- (29) Guo, C.; Shah, R. D.; Mills, J.; Dukor, R. K.; Cao, X.; Freedman, T. B.; Nafie, L. A. Fourier transform near-infrared vibrational circular dichroism used for on-line monitoring the epimerization of 2,2-dimethyl-1,3-dioxolane-4-methanol: a pseudo racemization reaction. *Chirality* **2006**, *18*, 775–782.
- (30) Jensen, A. A.; Brauner-Osborne, H. Pharmacological characterization of human excitatory amino acid transporters EAAT1, EAAT2 and EAAT3 in a fluorescence-based membrane potential assay. *Biochem. Pharmacol.* **2004**, *67*, 2115–2127.
- (31) Pople, J. A.; Schlegel, H. B.; Krishnan, R.; DeFrees, D. J.; Binkley, J. S.; Frisch, M. J.; Whiteside, R. A.; Hout, R. F.; Hehre, W. J. Molecular Orbital Studies of Vibrational Frequencies. *Int. J. Quantum Chem., Quantum Chem. Symp.* **1981**, *15*, 269–278.
- (32) Hout, R. F.; Levi, B. A.; Hehre, W. J. Effect of Electron Correlation on Theoretical Vibrational Frequencies. *J. Comput. Chem.* **1982**, *3*, 234–250.
- (33) Pople, J. A.; Head-Gordon, M.; Fox, D. J.; Raghavachari, K.; Curtiss, L. A. Gaussian-1 Theory: A General Procedure for Prediction of Molecular Energies. *J. Chem. Phys.* **1989**, *90*, S622–S629.
- (34) Curtiss, L. A.; Raghavachari, K.; Trucks, G. W.; Pople, J. A. Gaussian-2 Theory for Molecular Energies of First- and Second-Row Compounds. *J. Chem. Phys.* **1991**, *94*, 7221–7230.
- (35) Curtiss, L. A.; Carpenter, J. E.; Raghavachari, K.; Pople, J. A. Validity of additivity approximations used in Gaussian-2 theory. *J. Chem. Phys.* **1992**, *96*, 9030–9034.